Change of Colloidal and Surface Properties of Mytilus edulis Foot Protein 1 in the Presence of an Oxidation (NaIO(4)) or a Complex-Binding (Cu(2+)) Agent

ARTICLE *in* BIOMACROMOLECULES · FEBRUARY 2009

Impact Factor: 5.75 · DOI: 10.1021/bm801325j · Source: PubMed

Change of Colloidal and Surface Properties of *Mytilus edulis* Foot Protein 1 in the Presence of an Oxidation ($NaIO_4$) or a Complex-Binding (Cu^{2+}) Agent

J. Hedlund,[†] M. Andersson,[†] C. Fant,[†] R. Bitton,[‡] H. Bianco-Peled,[‡] H. Elwing,[†] and M. Berglin*,[†]

Department of Cell and Molecular Biology, Interface Biophysics, Göteborg University, Box 462, 405 30 Göteborg, Sweden, and Department of Chemical Engineering, Technion - Israel Institute of Technology, Haifa 32000 Israel

Received November 17, 2008; Revised Manuscript Received January 9, 2009

Quartz crystal microbalance with dissipation monitoring (QCM-D) was used to study the viscoelastic properties of the blue mussel, *Mytilus edulis*, foot protein 1 (Mefp-1) adsorbed on modified hydrophobic gold surfaces. The change in viscoelasticity was studied after addition of Cu^{2+} and Mn^{2+}, which theoretically could induce metal complex formation with 3,4-dihydroxyphenylalanine (DOPA) moieties. We also used $NaIO_4$, a nonmetal oxidative agent known to induce di-DOPA formation. Reduction in viscoelasticity of adsorbed Mefp-1 followed the order of $NaIO_4$ > Cu^{2+} > buffer control > Mn^{2+}. We also studied the formation of molecular aggregates of Mefp-1 in solution with the use of dynamic light scattering (DLS). We found that addition of Cu^{2+}, but not Mn^{2+}, induced the formation of larger DLS-detectable aggregates. Minor aggregate formation was found with $NaIO_4$. With the analytical resolution of small angle X-ray scattering (SAXS), we could detect differences in the molecular structure between $NaIO_4$- and Cu^{2+}-treated Mefp-1 aggregates. We concluded from this study that Cu^{2+} could participate in intermolecular cross-linking of the Mefp-1 molecule via metal complex formation. Metal incorporation in the protein most likely increases the abrasion resistance of the Mefp-1 layer. $NaIO_4$, on the other hand, resulted in mainly intramolecular formation of di-DOPA, but failed to induce larger intermolecular aggregation phenomena. The described methodological combination of surface sensitive methods, like QCM-D, and bulk sensitive methods, like DLS and SAXS, generates high resolution results and is an attractive platform to investigate intra- and intermolecular aspects of assembly and cross-linking of the Mefp proteins.

Introduction

Many sessile marine organisms are remarkable because they adhere to surfaces in a dirty and wet environment. The common blue mussel, *Mytilus edulis*, uses byssus threads that allows it to attach to hard surfaces in the sea.[1] The byssus consists of at least six polyphenolic proteins (Mefp1−6) with different functionalities and three collagenous proteins, with the former presumably acting as the adhesive and the latter as fibrous filler.[2] A common feature of all the polyphenolic proteins is that they contain a high content of the amino acid 3,4-dihydroxyphenyl-L-alanine (DOPA), which is generally attributed to their capacity to compete successfully with water at the surface and cross-link under water.[3−6] Mefp-1 was discovered by Waite and Tanzer, who extracted and purified an acid-soluble protein from the phenol gland located in the byssus-secreting foot of the blue mussel.[7] Mefp-1 is localized to the cuticle covering the outer surface of the adhesive plaque and byssus and it serves to protect underlying structural components from wear and microbial attack.[8] The protein has a molecular weight of ∼110 kD and is composed of a tandemly repeated decapeptide with up to 80 repeats. The repeat is highly basic and hydrophilic and DOPA occurs as often as twice in every repeat, which gives Mefp-1 a DOPA content of about 10−15%.[9]

The assembly at surfaces and curing (cross-linking) of the DOPA-containing Mefp-proteins is very complex and are not fully understood. There are numerous suggestions of potential cross-linking agents of the DOPA containing byssus proteins. Thus, enzymes, chemical oxidants and metal ions seem to take part in the cross-linking of Mefp proteins.[1,4,10−15] One striking feature of the byssus is the hundred fold higher concentrations of metal ions, for example, those of iron, zinc, copper, and manganese, compared to that of the surrounding seawater.[16] DOPA could hypothetically form metal complexes (chelating) with many of those metal ions, which may be one of the explanation to the high cohesive and adhesive strength of the Mefp proteins. The DOPA functionality is very sensitive to oxidation, and nonmetal oxidation agents such as $NaIO_4$ can also be used in the laboratory to induce cross-linking.[12,17] Monahan and Wilker made a survey of the effect of different metal salts and/or oxidative agents on DOPA-containing Mefp-1 and Mefp-2.[18] In this study they used a penetration test of the extracted gelatinous materials from the foot of the blue mussel. The results of the method were reproducible and they found that several nonmetal oxidizing agents such as $NaIO_4$ had a significant effect on the viscosity of the Mefp extract. Curing could also be explained by the chelating action of several metal ions. They concluded that "the Mefp-proteins are likely to employ compounds that have a combination of high degree of both oxidative properties and complex binding properties". Mn and Fe were therefore suggested, by these authors, as agents for cross-linking of the byssus proteins.

* To whom correspondence should be addressed. E-mail: mattias.berglin@cmb.gu.se.
[†] Göteborg University.
[‡] Technion - Israel Institute of Technology.

10.1021/bm801325j CCC: $40.75
Published on Web 02/11/2009

The aim of the present investigation was to investigate curing or cross-linking phenomena of Mefp-1 protein with the use of quartz crystal microbalance with dissipation monitoring (QCM-D). The QCM-D technique is a simple, high-resolution mass sensing technique, based upon the piezoelectric effect of quartz. The method can be used to detect monolayer surface coverage by protein molecules or polymer films, often in the ng/cm^2 range.[19] Besides mass-determination (frequency, or f-parameter), there is also a possibility to detect the viscoelastic properties (dissipation or D-parameter) of adsorbed molecules.[20,21] We have previously used the methodology to study cross-linking of Mefp-1 and other marine adhesive polymers.[12,20,22] In this study the focus was on the shift in dissipation to better reveal molecular and structural changes upon curing.

We combined the QCM-D studies with dynamic light scattering (DLS) and small angle X-ray scattering (SAXS), which are two bulk sensitive methods. By employing these methods, we hope to differentiate between inter- and intramolecular cross-linking. As curing or cross-linking agent, we used $NaIO_4$, which is not likely to result in complex binding with DOPA despite being a strong oxidizing agent. We also used Cu^{2+} and Mn^{2+}, both found in high concentrations in the byssus threads of selected mussel species, and hypothetically could take part in complex formation with DOPA.[23,24] The ions Cu^{2+} and Mn^{2+} will not likely oxidize DOPA in the pH range we used.

Materials and Methods

Mefp-1. Mefp-1 (Biopolymer Products AB, Alingsås, Sweden) was diluted to 0.025 mg/mL in 0.1 M acetate buffer (0.075 M NaCl, pH 5.5). Both acetate buffer and sodium chloride was provided by Sigma-Aldrich, Sweden. The pH of the acetate buffer is below the upper limit at which Mefp-1 undergoes spontaneous oxidation and subsequent cross-linking/aggregation in solutions.

Quartz Crystal Microbalance with Dissipation Monitoring (QCM-D). The instrument used was a D-300 apparatus from Q-sense AB, Sweden. The analysis was done in a measurement chamber designed to provide a fast nonperturbing exchange of a stagnant liquid. The measurement chamber was temperature-stabilized to 22 ± 0.02 °C. Prior to use $NaIO_4$ (1 mM), $CuCl_2$ (10 mM), and $MnCl_2$ (10 mM) was diluted in 0.1 M acetate buffer (0.075 M NaCl, pH 5.5). Mefp-1 (0.025 mg/mL) in acetate buffer was allowed to adsorb for 50 min, followed by a rinse in acetate buffer for 5 min. The oxidizing agent or metal ions was added for 15 min, followed by a final rinse in acetate buffer for 5 min. It should be stressed that iron ($FeCl_3$) was considered for the studies but reproducible results could not be obtained. Moreover, we regularly observed a precipitate in the Fe^{3+} solutions. To prevent any bias in the results due to this irreproducibility and precipitate formation the results with Fe^{3+} was omitted in this paper.

One-factor analysis of variance (ANOVA, significance level 0.05) was performed on the data, where the relative change in dissipation (ΔD) for each treatment was measured with QCM-D. Five replicates were done for each treatment. A manual posthoc test was done to distinguish between which groups there were a significant difference in ΔD.

Gold coated QCM-D sensor surfaces (Q-sense AB, Göteborg, Sweden) were cleaned in a UV chamber for 10 min and then immersed in a mixture of H_2O_2 (Sigma-Adrich, Sweden), NH_3 (VWR, Sweden), and milli-Q water for 5 min at 70 °C. To obtain a chemically well-defined, electrically inert, and nonpolar surface, the gold-coated crystals were immersed for more than 12 h in a solution of an 18-carbon alkane thiol (Aldrich, Germany) with a -CH_3 end group ($HS(CH_2)_{17}CH_3$) dissolved in hexane (Sigma-Aldrich, Sweden). The quality of the hydrophobic self-assembled monolayer was checked with static contact angle measurements.[25] A 10 μL drop of milli-Q water was placed on the hydrophobically modified surface and when equilibrium was reached the angle between surface and water drop was measured with a goniometer fitted to a microscope. A contact angle of 90° and higher was accepted.

Dynamic Light Scattering (DLS). DLS measurements were performed using a BI-200SM Research Goniometer System (Brookhaven Instruments Corp., U.S.A.). A Compass 415 M solid-state laser (Coherent, U.S.A.), generating monochromatic green light of 532 nm wavelength, was used. The detector assembly includes a selected photomultiplier tube (PMT), diode chain, and an integral amplifier/discriminator. The BI-9000AT digital signal processor (Brookhaven Instruments Corp., U.S.A.) was used as a correlator for DLS measurements. Samples were placed in a 45 mm tall, 6 × 6 mm rectangular quartz cell with Teflon cap, immersed in a glass vat containing decalin as the index-matching fluid. The recorded autocorrelation functions where analyzed using an inverse Laplace transform (CONTIN procedure)[26] using a software provided with the instrument. This analysis gave the value of the hydrodynamic radius R_h.

Small Angle X-ray Scattering (SAXS). SAXS measurements were performed using a slit-collimated compact Kratky camera (A. Paar Co., Austria). The entrance slit to the collimating block was 20 m, and the slit length delimiters were set at 15 mm. Ni filtered Cu Kα (1.542 Å) radiation was generated by a sealed tube (Philips, U.S.A.). Samples were placed in cylindrical quartz cells (A. Paar Co., Austria, 2 mm path length), and their temperature was kept constant by means of a temperature controller (A. Paar Co., Austria) at 25 °C. The sample to detector distance was 26.4 cm, and the flight path was kept under vacuum. Scattering was measured with a linear position sensitive detector system (Raytech, France, gold-coated tungsten wire in a stream of 90% Ar + 10% CH_4 gas at 3 bar), with pulse-height discrimination and a multichannel analyzer (Nucleus, U.S.A.). A total of 3000 or more counts for each channel were collected to obtain a low signal-to-noise ratio. Primary beam intensities were determined using the moving slit method of Stabinger and Kratky[27] and subsequently using a thin quartz monitor as a secondary standard. The scattering curves, as a function of the scattering vector, $q = 4\pi \sin \theta/\lambda$ (where 2θ and λ are the scattering angle and the wavelength, respectively), were corrected for counting time and for sample absorption. The background scattering was measured separately and subtracted from the scattering curve. To rectify the effects of the beam dimensions, a desmearing procedure was performed according to the indirect transformation method using the method provided in the reference by Glatter.[28] The indirect transformation method is one of the most popular methods for obtaining real-space information from small-angle scattering data. In particular, the method is used to desmear those SAXS curves where interparticle interference effects are present, with the aim of obtaining the interference function. Data analysis was based on fitting the desmeared curve to an appropriate model using a least-squares procedure.

Results and Discussion

In Figure 1, representative graphs of the shift in dissipation as a function of treatment and the acetate buffer control are shown. The average shift in dissipation for all treatments is summarized in Figure 2. The one-factor ANOVA analysis of data showed that there is a significant difference in dissipation between treatments and the posthoc test showed that the decreases in dissipation for all treatments are significantly different from each other. Both $NaIO_4$ and Cu^{2+} induced rapid structural changes but no dramatic changes were observed with Mn^{2+} and control (Figure 1). $NaIO_4$ mimics one potential curing mechanism, that is, the enzymatic cross-linking via catechol oxidase. Catechol oxidase present in the byssus could oxidize available DOPA residues to highly reactive *o*-quinones. The *o*-quinones are capable of inducing cross-linking in the polyphenolic proteins by the formation of di-DOPA cross-links (Figure 3), suggested previously.[4,6,29]

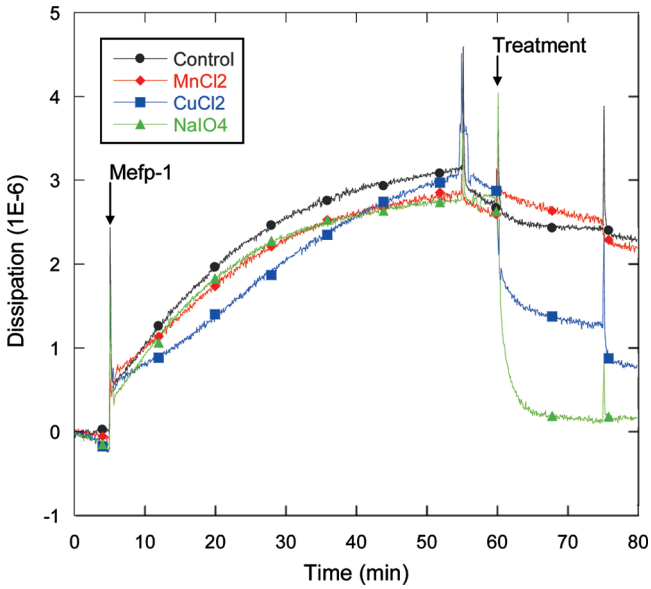

Figure 1. Representative QCM-D measurements for the different treatments. Structural changes upon addition of the agents are indicated as a decrease in dissipation. The lines in the graph are represented in the following order: $MnCl_2$ (red diamond), control (black circle), $CuCl_2$ (blue square), and $NaIO_4$ (green diamond). The largest shift in dissipation is induced by $NaIO_4$, while Cu induces an intermediate decrease. The control (buffer only) and Mn-treated samples did not alter the viscosity of the adsorbed Mefp-1 film.

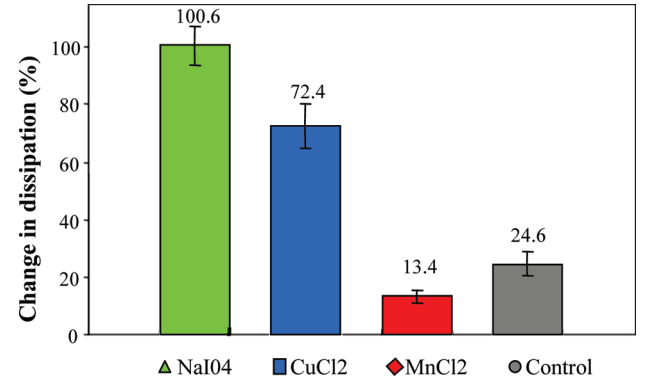

Figure 2. The average decrease in dissipation (%) for adsorbed Mefp-1 treated with $NaIO_4$, $CuCl_2$, $MnCl_2$, and buffer (control). Addition of $NaIO_4$ transforms the adsorbed protein film to the most rigid state of all agents. Cu, which is known to form complexes with DOPA, induces an intermediate response (74.2 ± 8%). Small changes were observed with Mn and control group.

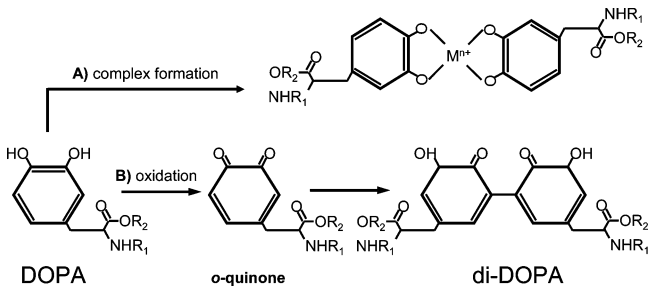

Figure 3. Possible reaction pathways for cross-linking of DOPA. (A) Complex formation between transition metal ions and DOPA. (B) Formation of di-DOPA cross-links.

The structural changes reflected in decreased dissipation upon introduction of Cu^{2+} could be due to a DOPA−Cu−DOPA complex formation (Figure 3). Another explanation could be that Cu^{2+} induces oxidation of the DOPA to *o*-quinones followed by di-DOPA formation, similar to the mechanism discussed above. To distinguish between the two mechanisms electron paramagnetic resonance (EPR) could be used. However, the decrease in dissipation upon treatment with Cu^{2+} is lower than when using $NaIO_4$, which is indicating differences in structural changes between the two. Cu^{2+} is known to interact with DOPA[23] and have been found in the byssus of some mussel species.[30,31] Interesting to note is that Mn^{2+}, which also has been found in the byssus,[16] causes even less dissipation change than the control. Thus, there seems to be no complex formation or oxidation with this metal ion. The change in dissipation in the control group is probably due to some desorption of the Mefp-1 proteins upon rinsing.

Experiments using Fe^{3+} was also carried out but the reproducibility was poor (data not presented). One likely explanation could be that Fe^{3+} is able to form DOPA−Fe−DOPA complexes and oxidize DOPA to reactive *o*-quinones, which then form covalent cross-links. In one report, self-assembled monolayers were constructed with terminal hydroquinone residues designed to model marine adhesive proteins.[32] With cyclic voltametry the hydroquinone oxidation was shifted by −440 mV at pH 5 for Fe^{3+} solutions. Thus, the DOPA functionality becomes much more easily oxidized in the presence of Fe^{3+} even at low pH. Synergistic effects between oxidants and metal ions were also recently observed by Lauren and Wilker.[33] Curing of the mussel adhesives are probably not so simple that only one primary mechanism controls the cross-linking reaction, but the reaction is dictated by the fine-tuned interplay between metal complex formation and oxidation.

Monahan and Wilker[18] studied the shift in viscosity of a mixture of Mefp proteins using a vide range of different oxidation agents. They studied the bulk properties by measuring the average penetration force needed to penetrate into the Mefp solution after treatment. The result from this study does coincide with our result that there is a decreasing degree of curing with $NaIO_4$, Cu^{2+}, and Mn^{2+} respectively. However, the main difference in their study was between $NaIO_4$ and the metal ions. The large difference in dissipation shift observed between the metals in our study, Cu^{2+} and Mn^{2+}, need some attention. We both used proteins prepared from *Mytilus edulis* for the experiments so interspecies differences are not present. One likely explanation is that the mixture of mussel adhesive proteins present in the preparation by Wilkner makes cross-link formation with Mn^{2+} possible. Thus, different Mefp proteins could use different ions for the metal complex formation.

The uptake of metals is an active process where the byssus might serve as a disposal system for toxic metal ions.[34,35] Metal accumulation may also be a consequence of the high levels of DOPA in the byssus and serve as a cross-linking pathway coexisting with the enzymatically formation of di-DOPA cross-links. In a recent paper, Holten-Andersen et al. showed increased levels of Fe and Ca in the byssus cuticle from the mussel *Mytilus galloprovincalis*.[36] They also showed that this metal incorporation lead to 2-fold elevations in the hardness. Thus, it is evident that complex formation between DOPA and metal ions will contribute with increased cohesive strength and abrasion resistance in the byssus.

DLS measurements provide additional support to the suggestion that the studied agents, the metal ions and $NaIO_4$, interacted with Mefp-1 in a different manner. The hydrodynamic radius of the native Mefp-1 does not change in the presence of Mn^{2+} (Figure 4), supporting the claim that this ion does not lead to intermolecular DOPA cross-linking. The hydrodynamic radius of our Mefp-1 control sample is somewhat smaller, but

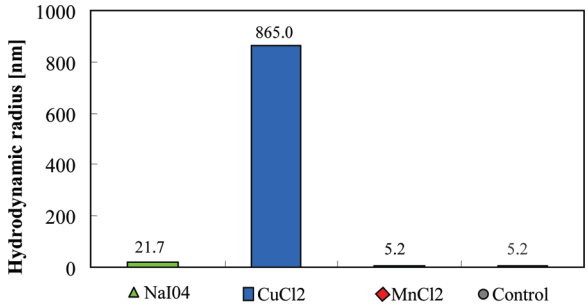

Figure 4. Results of the CONTIN analysis for hydrodynamic radius of Mefp-1 treated with $NaIO_4$, $CuCl_2$, $MnCl_2$, and buffer. The Mefp-1 concentration was 0.7 mg/mL.

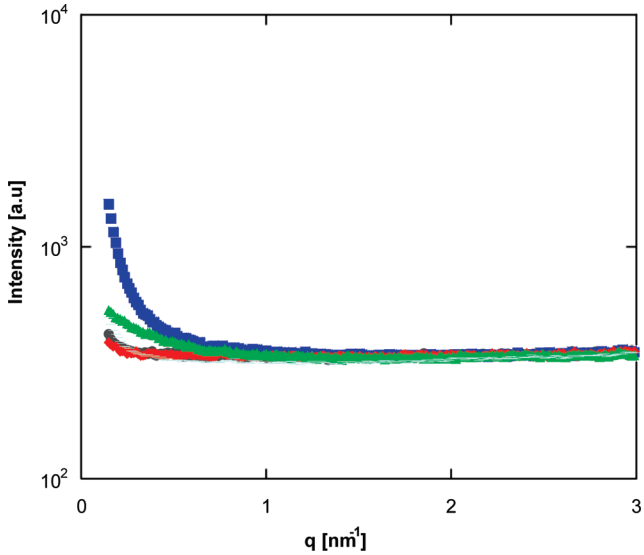

Figure 5. Small-angle X-ray scattering from water (green line), Mefp-1 oxidized with $NaIO_4$ (green triangle), $CuCl_2$ (blue square), $MnCl_2$ (red diamond), and buffer only (black circle).

in the same order, as those reported by Haemers and co-workers.[37] One explanation for the difference could be that Haemers et al. measured the hydrodynamic radius under physiological conditions while we made the measurements at lower pH. As we both received Mefp-1 from the same producer, differences due to different preparation protocols should be minimal. It can be speculated that our protein was somewhat degraded prior to the study. However, it does not alter the finding that Mn^{2+} is not able to form DOPA−Mn−DOPA cross-links with the Mefp-1 protein.

In contrast, $NaIO_4$ and Cu^{2+} induce aggregation of the Mefp-1 molecules, as revealed from the increased hydrodynamic radius. Interestingly, aggregates formed due to Cu^{2+} are much larger than those found in $NaIO_4$ treated solutions. The small aggregate size in the case of $NaIO_4$ treatment indicates that much of the di-DOPA formation could be between different DOPA moieties in the same Mefp-1 molecule (intracross-link formation). However, it should be stressed that kinetic reactions of macromolecules bearing reactive groups are unusual in many aspects. They not only depend on the chemical reaction rates, but also on the dynamics and the conformation of the macromolecules. Moreover, molecular weight, solvent, concentration, and chain stiffness is likely to affect the kinetics. We used a rather low concentration compared with for example Haemers et al.[37] Using higher concentration might have resulted in larger Mefp-1 aggregates. Consequently, the results obtained with $NaIO_4$ should be viewed with these factors in mind.

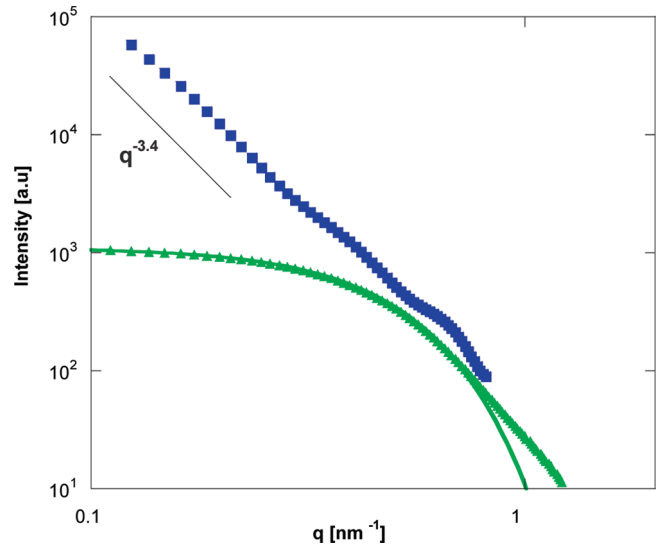

Figure 6. Background subtracted SAXS curve Mefp-1 oxidized with $NaIO_4$ (green triangle) and $CuCl_2$ (blue square). The solid line represents a fit according to a Guinier approximation eq 1.

SAXS experiments were performed in an attempt to study details of the molecular structure of Mefp-1 aggregates. However, since the nonoxidized Mefp-1 does not display excess scattering, its structural features cannot be analyzed (Figure 5). Nevertheless, the SAXS measurements provide additional experimental support to our previous conclusions. First, the scattering from the nonoxidized Mefp-1 and from Mefp-1 oxidized with Mn^{2+} are identical, again supporting that the Mn^{2+} does not induce any DOPA cross-linking. However, the presence of $NaIO_4$ and Cu^{2+} seem to alter the nanostructure dramatically. Treatment with either Cu^{2+} or $NaIO_4$ results in an upturn at the low-q regime, which indicates the presence of large aggregates in the sample. Yet, the apparent dissimilarity between the two scattering profiles implies that the aggregate's size and shape depends on the different agents. The differences are highlighted in a log−log plot of the background-subtracted scattering patterns presented in Figure 6.

The scattering pattern of the $NaIO_4$-treated samples was well fitted by the Guinier approximation in the low-q range, according to[28]

$$I = A \exp\left(\frac{R_g^2 q^2}{3}\right) \quad (1)$$

where A is a prefactor and R_g is the radius of gyration. The best fit yielded value of 3.7 nm ± 0.1 nm for the gyration radius. Note that the hydrodynamic radius, as measured with DLS, arises of the dynamic properties of polymers moving in a solvent. It is often similar in magnitude to the radius of gyration. The radius of gyration of 3.7 nm as determined with SAXS is much smaller that the hydrodynamic radius of 21.7 nm, determined with DLS. The discrepancy can be attributed to the low contrast between the Mefp-1 molecule and the buffer, which also explains the lack of excess scattering from the native protein.

Similar to $NaIO_4$, added Cu^{2+} gives rise to excess scattering. In this case, a $q^{-3.4}$ dependence was observed (Figure 6). The DLS detected formation of very large aggregates in this sample and a q^{-4} dependence could be expected. A possible explanation for the divergence may be due to ill-defined surfaces and sizes of the scattering objects.[38] We suggest that the structural feature observed by SAXS arise from higher-density domains due to local segregation of the metal ions.

Conclusions

The structural change or cross-linking of *Mytilus edulis* foot protein 1 (Mefp-1) upon treatment with Cu^{2+}, Mn^{2+}, and $NaIO_4$, was determined with QCM-D, DLS, and SAXS. As evidenced by the shift in dissipation and aggregate formation, we concluded that Cu^{2+} but not Mn^{2+} was able to induce intermolecular cross-links between different Mefp-1 molecules. Metal complex formation, that is, DOPA−metal ion−DOPA, was the most probable mechanism. With $NaIO_4$ we observed some intermolecular cross-link formation as evidenced by the shift to larger aggregates, but the greater part of the di-DOPA cross-links formed appeared to be within the Mefp-1 molecule (intramolecular cross-link formation). The described methodological combination of surface sensitive methods like QCM-D and bulk sensitive methods, like DLS and SAXS, generate high resolution results and is an attractive platform to investigate intra- and intermolecular aspects of assembly and cross-linking of the Mefp proteins.

Acknowledgment. We would like to thank Biopolymer Products AB, Sweden, for supplying the mussel adhesive protein, the MISTRA research program Marine Paint, and the EC research program Algal Bioadhesives (AB) for funding the research.

References and Notes

(1) Waite, J. H. *Int. J. Adhes. Adhes.* **1987**, *7*, 9–14.
(2) Waite, J. H. *Integr. Comp. Biol.* **2002**, *42*, 1172–1180.
(3) Weinhold, M.; Soubatch, S.; Temirov, R.; Rohlfing, M.; Jastorff, B.; Tautz, F. S.; Doose, C. *J. Phys. Chem. B* **2006**, *110*, 23756–23769.
(4) McDowell, L. M.; Burzio, L. A.; Waite, J. H.; Schaefer, J. *J. Biol. Chem.* **1999**, *274*, 20293–20295.
(5) Burzio, L. A.; Burzio, V. A.; Pardo, J.; Burzio, L. O. *Comp. Biochem. Phys. B* **2000**, *126*, 383–389.
(6) Burzio, L. A.; Waite, J. H. *Biochemistry* **2000**, *39*, 11147–11153.
(7) Waite, J. H.; Tanzer, M. L. *Science* **1981**, *212*, 1038–1040.
(8) Rzepecki, L. M.; Waite, J. H. *Mol. Mar. Biol. Biotechnol.* **1995**, *4*, 313–322.
(9) Vreeland, V.; Waite, J.; Epstein, L. *J. Phycol.* **1998**, *34*, 1–8.
(10) Crisp, D. J.; Walker, G.; Young, G. A.; Yule, A. B. *J. Colloid Interface Sci.* **1985**, *104*, 40–50.
(11) Inoue, K.; Takeuchi, Y.; Miki, D.; Odo, S. *J. Biol. Chem.* **1995**, *270*, 6698–6701.
(12) Fant, C.; Sott, K.; Elwing, H.; Hook, F. *Biofouling* **2000**, *16*, 119–132.
(13) Anderson, K. E.; Waite, J. H. *Biofouling* **2002**, *18*, 37–45.
(14) Yu, M. E.; Hwang, J. Y.; Deming, T. J. *J. Am. Chem. Soc.* **1999**, *121*, 5825–5826.
(15) Loizou, E.; Weisser, J. T.; Dundigalla, A.; Porcar, L.; Schmidt, G.; Wilker, J. J. *Macromol. Biosci.* **2006**, *6*, 711–718.
(16) Swann, C. P.; Adewole, T.; Waite, J. H. *Comp. Biochem. Physiol., Part B: Biochem. Mol. Biol.* **1998**, *119*, 755–759.
(17) Berglin, M.; Fant, C.; Hedlund, J.; Elwing, H. *J. Adhes.* **2005**, *81*, 805–822.
(18) Monahan, J.; Wilker, J. J. *Langmuir* **2004**, *20*, 3724–3729.
(19) Marx, K. A. *Biomacromolecules* **2003**, *4*, 1099–1120.
(20) Hook, F.; Kasemo, B.; Nylander, T.; Fant, C.; Sott, K.; Elwing, H. *Anal. Chem.* **2001**, *73*, 5796–5804.
(21) Rodahl, M.; Hook, F.; Kasemo, B. *Anal. Chem.* **1996**, *68*, 2219–2227.
(22) Berglin, M.; Delage, L.; Potin, P.; Viltner, H.; Elwing, H. *Biomacromolecules* **2004**, *5*, 2376–2383.
(23) Suzuki, S.; Yamaguchi, K.; Nakamura, N.; Tagawa, Y.; Kuma, H.; Kawamoto, T. *Inorg. Chim. Acta* **1998**, *283*, 260–267.
(24) Albrecht, M. *Chem. Soc. Rev.* **1998**, *27*, 281–287.
(25) Garbassi, F.; Morra, M.; Occhiello, E., *Polymer Surfaces, From Physics to Technology*; John Wiley & Sons Ltd: Chicester, 1994.
(26) Provencher, S. W. *Biophys. J.* **1976**, *16*, 27–41.
(27) Stabinger, H.; Kratky, O. *Makromol. Chem.* **1978**, *179*, 1655–1659.
(28) Glatter, O. *J. Appl. Crystallogr.* **1977**, *10*, 415–421.
(29) Haemers, S.; van der Leeden, M. C.; Koper, G. J. M.; Frens, G. *Langmuir* **2002**, *18*, 4903–4907.
(30) Gundacker, C. *Chemosphere* **1999**, *38*, 3339–3356.
(31) Kadar, E.; Bettencourt, R. *Biometals* **2008**, *21*, 395–404.
(32) Brooksby, P. A.; Schiel, D. R.; Abell, A. D. *Langmuir* **2008**, *24*, 9074–9081.
(33) Lauren, M. H.; Wilker, J. J. *J. Mater. Sci.* **2007**, *42*, 8934–8942.
(34) Szefer, P.; Kim, B. S.; Kim, C. K.; Kim, E. H.; Lee, C. B. *Environ. Pollut.* **2004**, *129*, 209–228.
(35) Szefer, P.; Frelek, K.; Szefer, K.; Lee, C. B.; Kim, B. S.; Warzocha, J.; Zdrojewska, I.; Ciesielski, T. *Environ. Pollut.* **2002**, *120*, 423–444.
(36) Holten-Andersen, N.; Mates, T. E.; Toprak, M. S.; Stucky, G. D.; Zok, F. W.; Waite, H. J. *Langmuir* **2008**, DOI: 10.1021/la8027012.
(37) Haemers, S.; van der Leeden, M. C.; Frens, G. *Biomaterials* **2005**, *26*, 1231–1236.
(38) Buhler, E.; Boue, F. *Macromolecules* **2004**, *37*, 1600–1610.

BM801325J